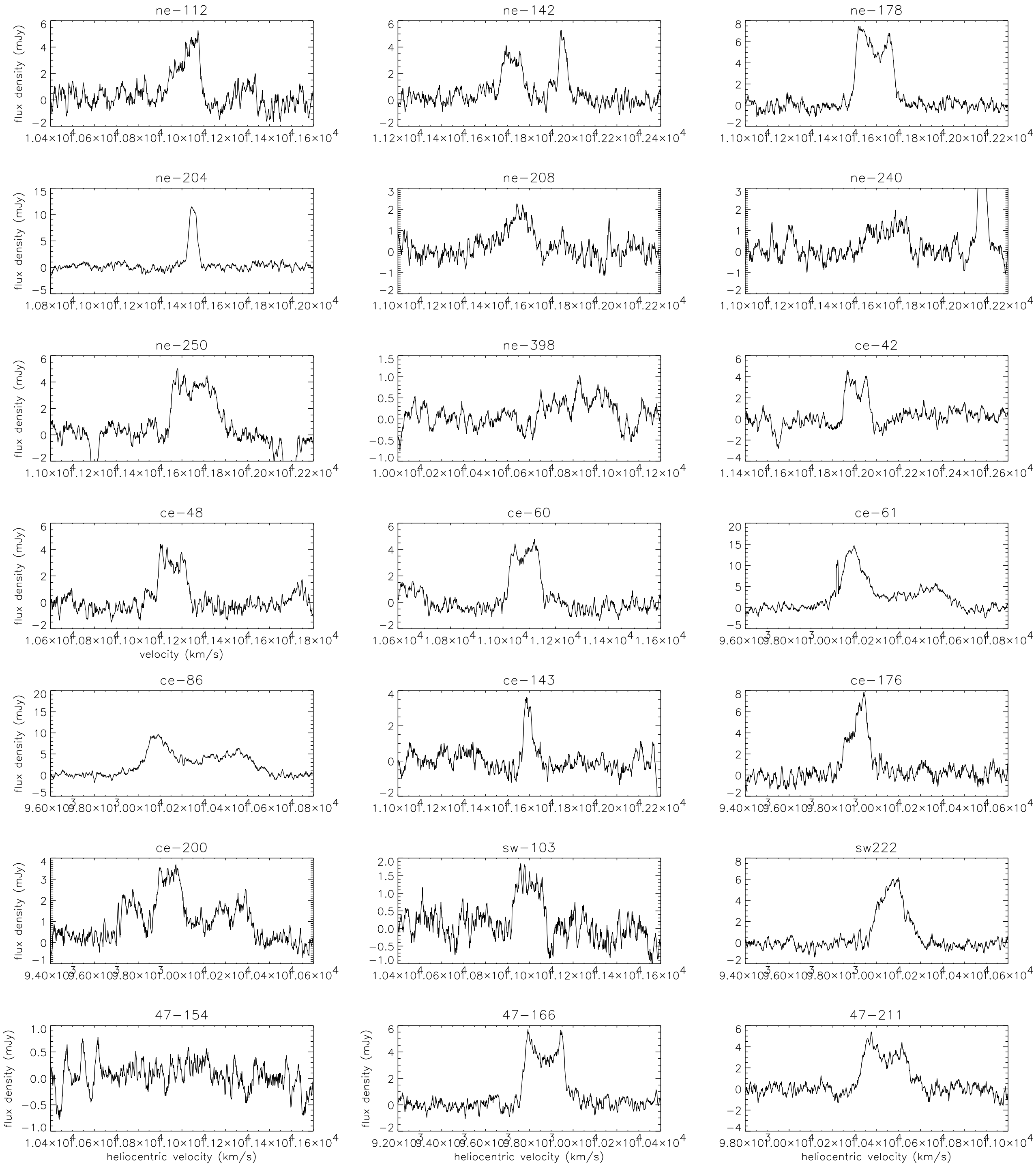

Fig. 1. Arecibo 21 cm H I line spectra of 20 galaxies in the Hercules cluster; for details on the ce-61 and ce-86 sources, see comments on ce-061 (Appendix A). The velocity resolution of the data is 9.1 $\mathrm{km\,s^{-1}}$ for most spectra, and 19.4 $\mathrm{km\,s^{-1}}$ for ne-398 and 47-154.

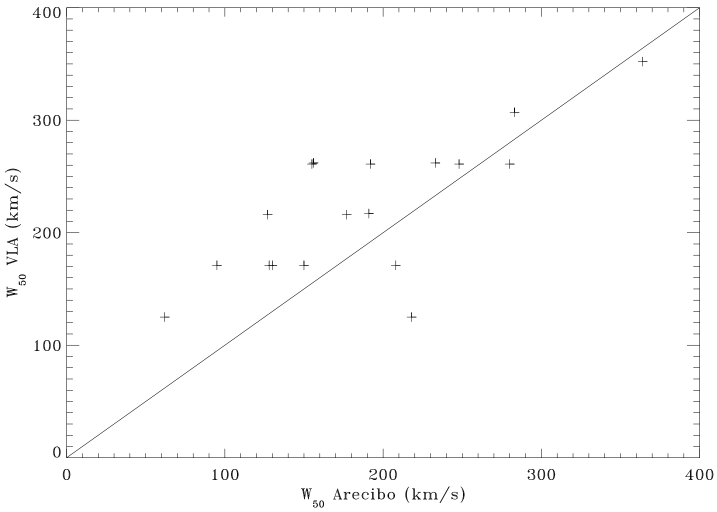

Fig. 2. Comparison of W_{50} line widths of integrated H I profiles measured at Arecibo and the VLA, see the text for details.

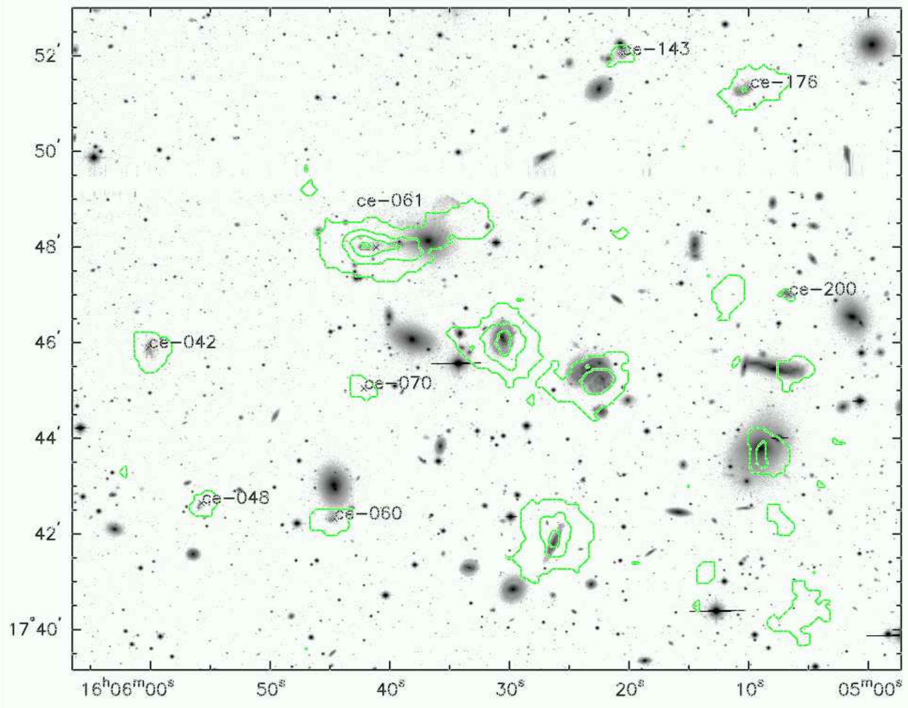

Fig. 3. (a) VLA H I column density contours superposed on our optical V-band image of field ce. The labels indicate the H I-selected galaxies in this field. R.A. and Dec. are in J2000.

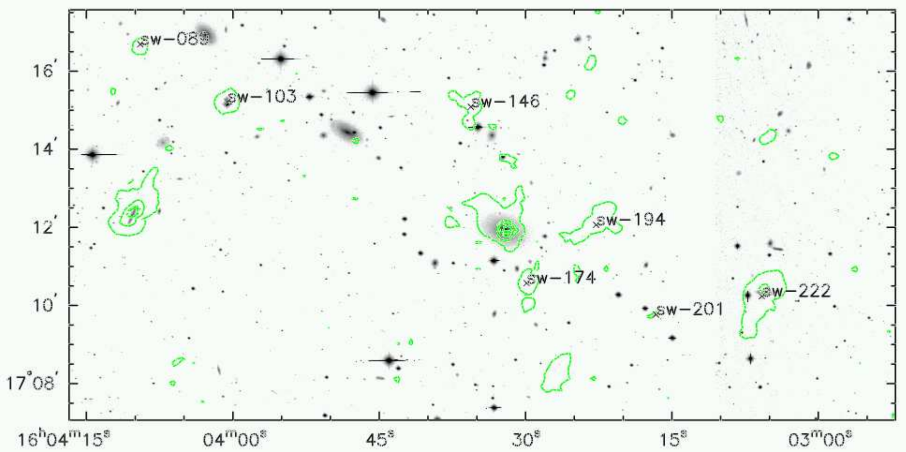

Fig. 3. (b) VLA H I column density contours superposed on our optical V-band image of field sw. The labels indicate the H I-selected galaxies in this field. R.A. and Dec. are in J2000.

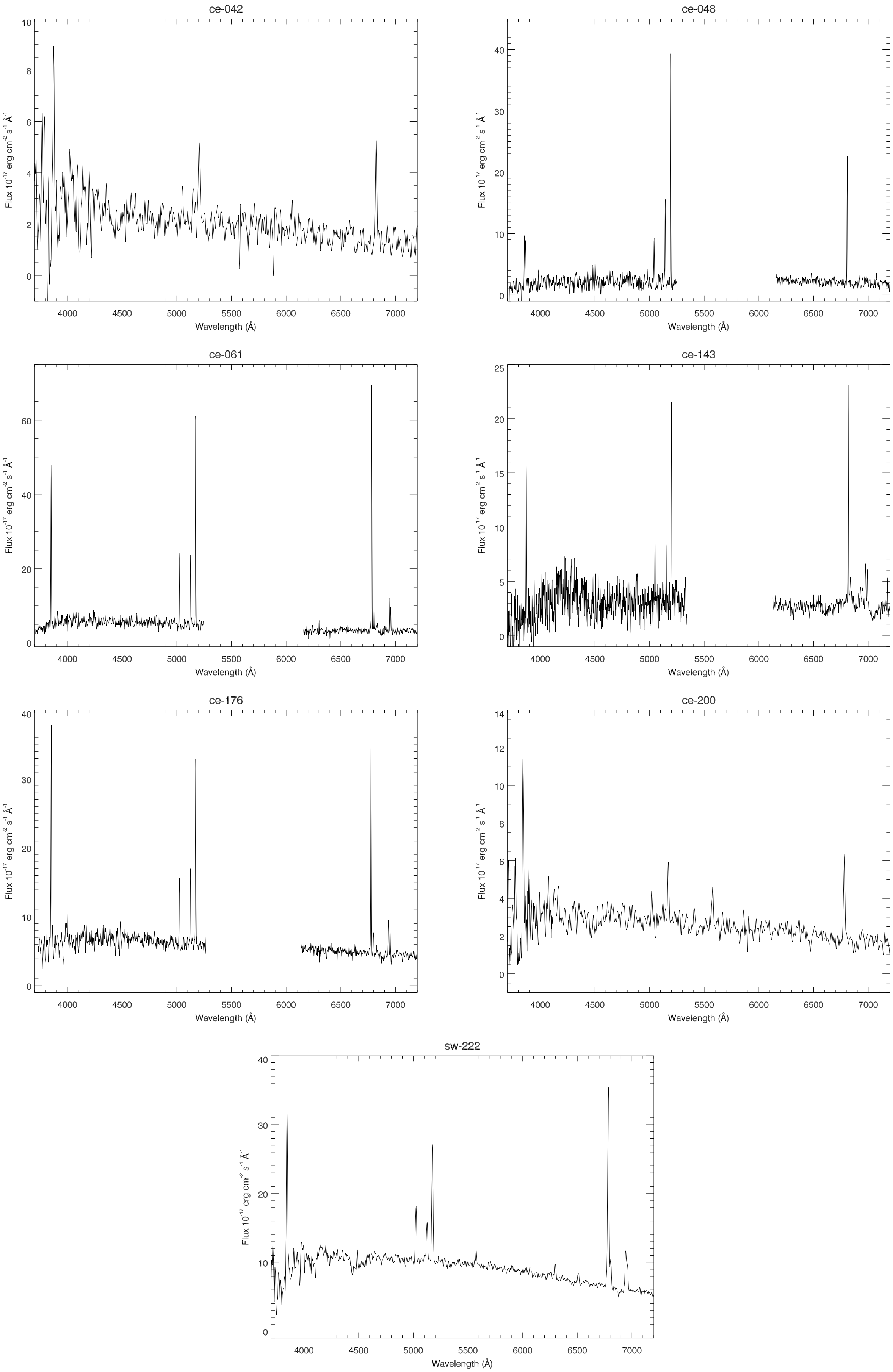

Fig. 4. Optical spectra of the seven galaxies showing emission lines.

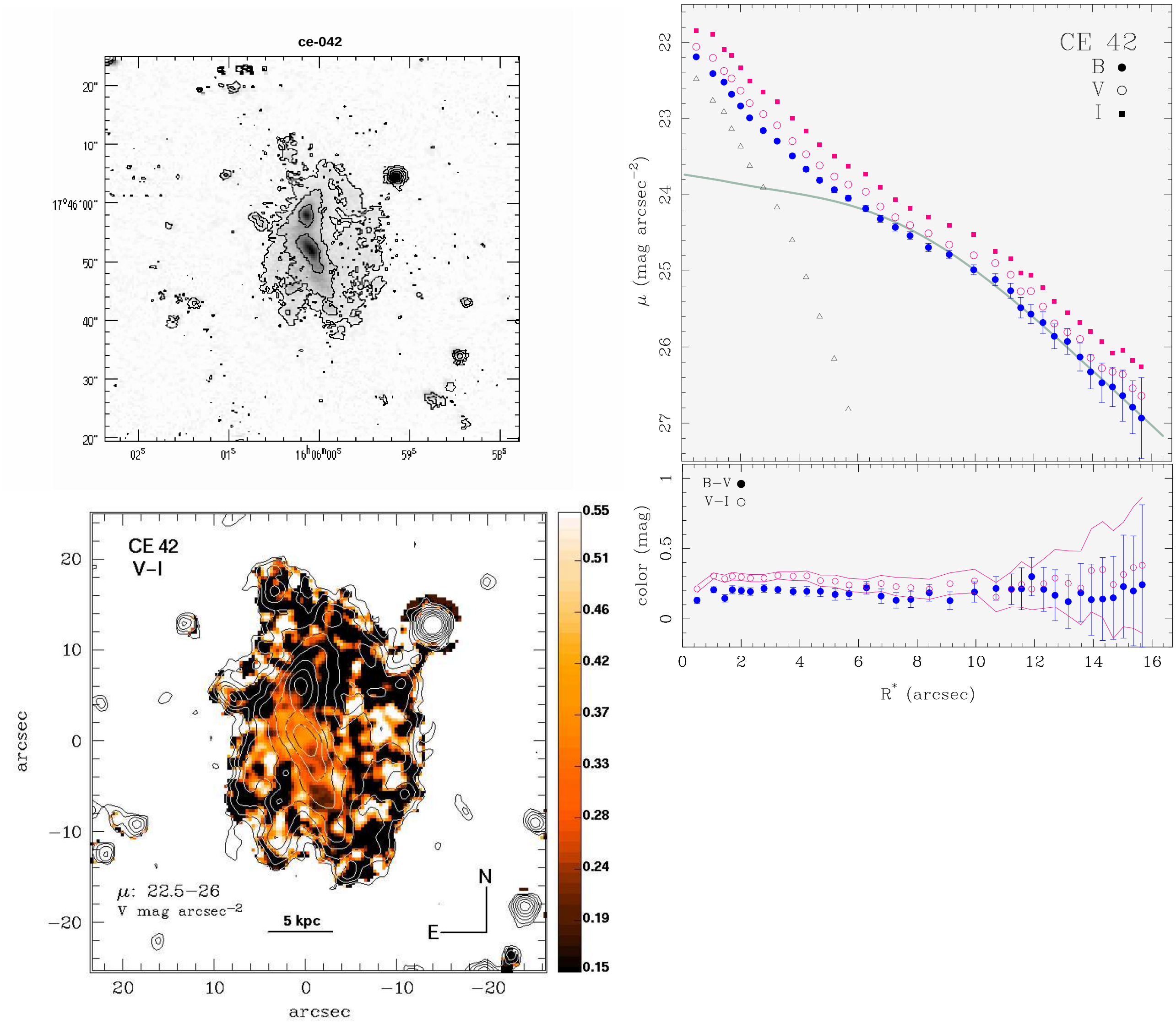

Fig. 5. Photometric properties of ce-042: **Upper left:** V-band image with superposed contour plots at 25.5, 24.5, 23.5, 22.5 and 21.5 mag arcsec^{-2}. The coordinates are in J2000.0 **Lower left:** $(V - I)$ colour map with V-band contours superposed **Upper right:** Surface brightness profiles. The fitted surface brightness distribution of the LSB component in B is depicted by the thick/grey curve. Open triangles show the emission in excess to the LSB component **Lower right:** Colour profiles

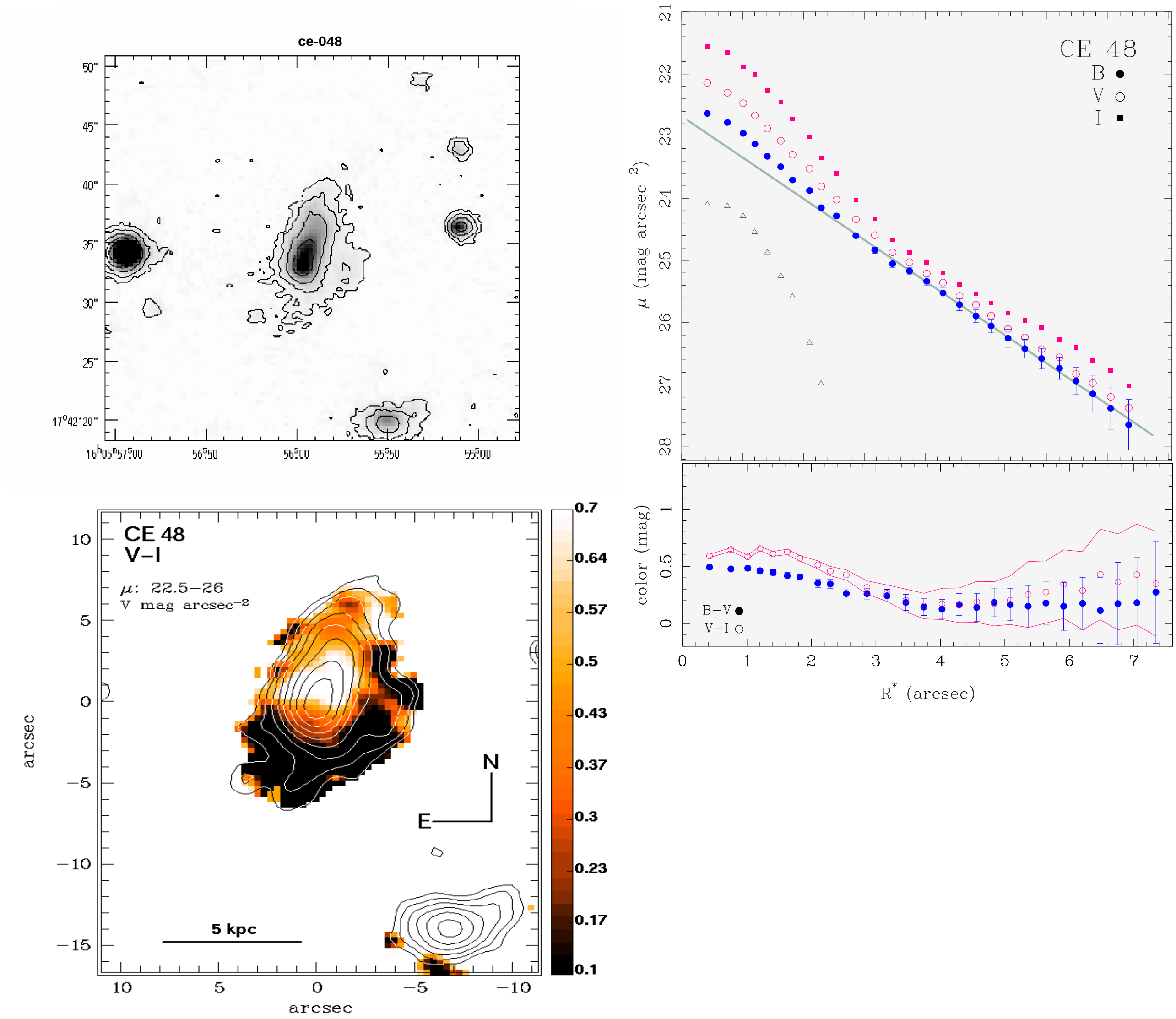

Fig. 6. Same as Figure 5 for ce-048

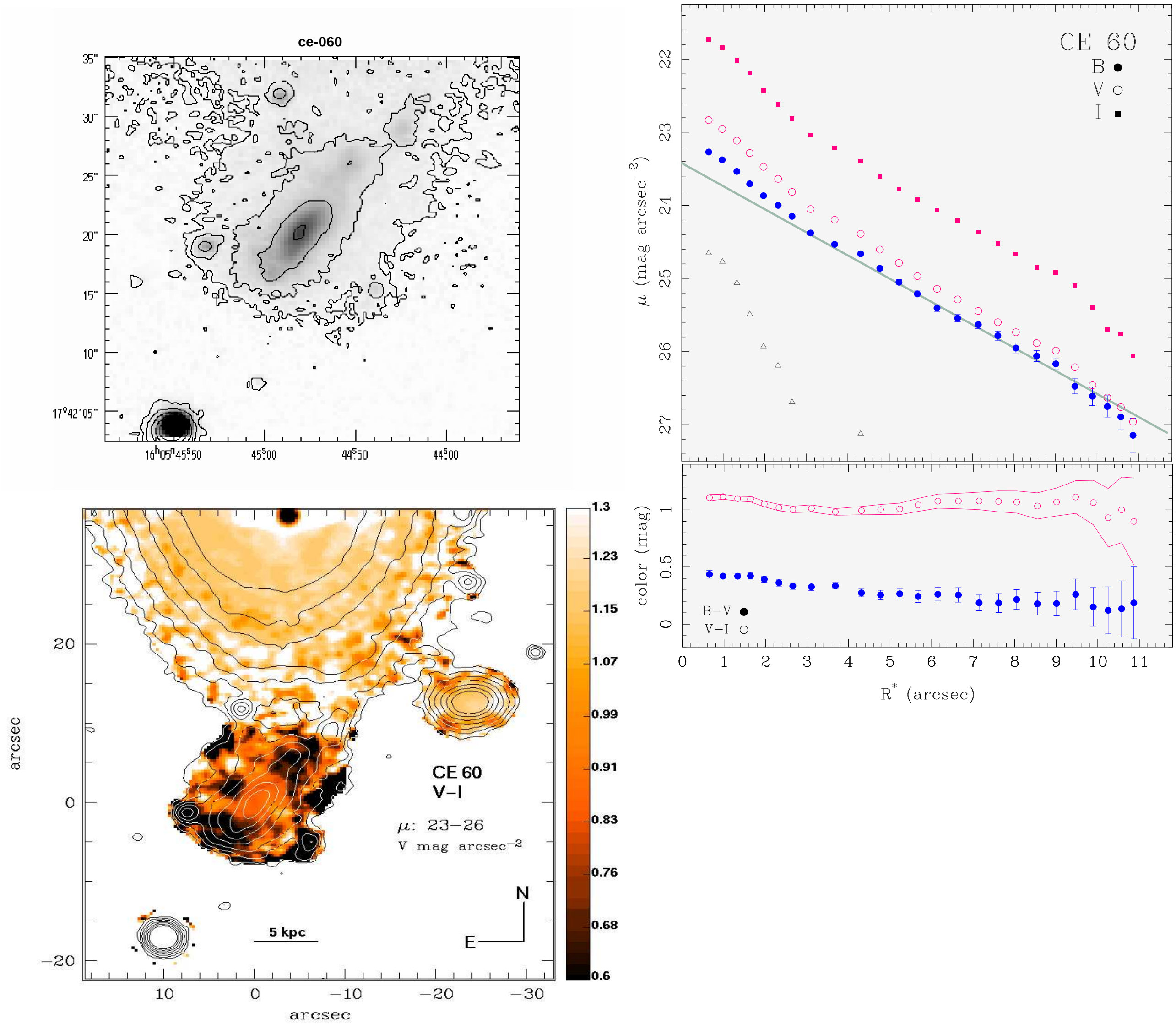

Fig. 7. Same as Figure 5 for ce-060

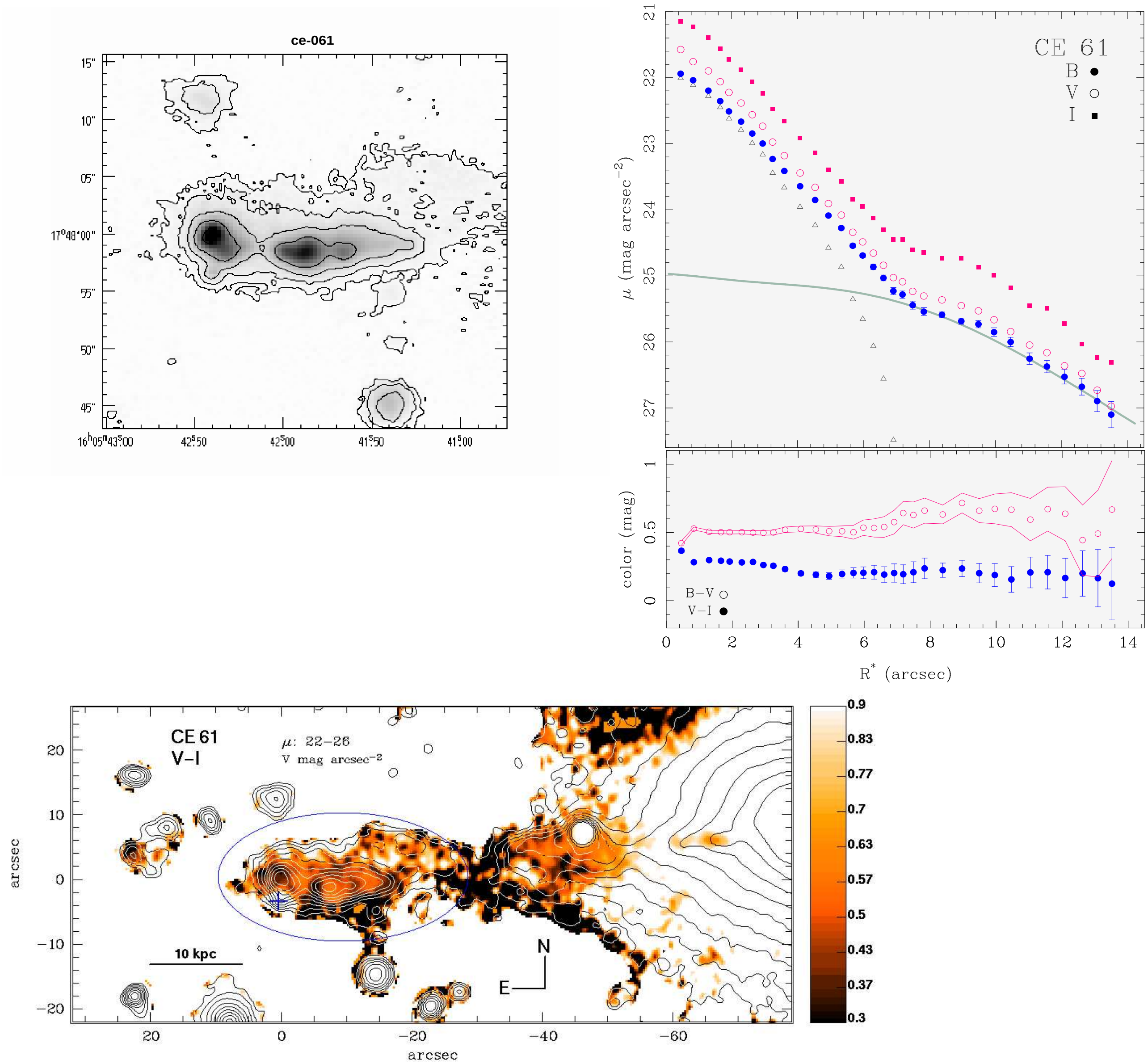

Fig. 8. Same as Figure 5 for ce-061. The ellipse indicates the segment of tidal tail included in the surface photometry analysis. The small crosses in the maps show a red point like sources (probably a foreground star) which was removed before computing the SBPs.

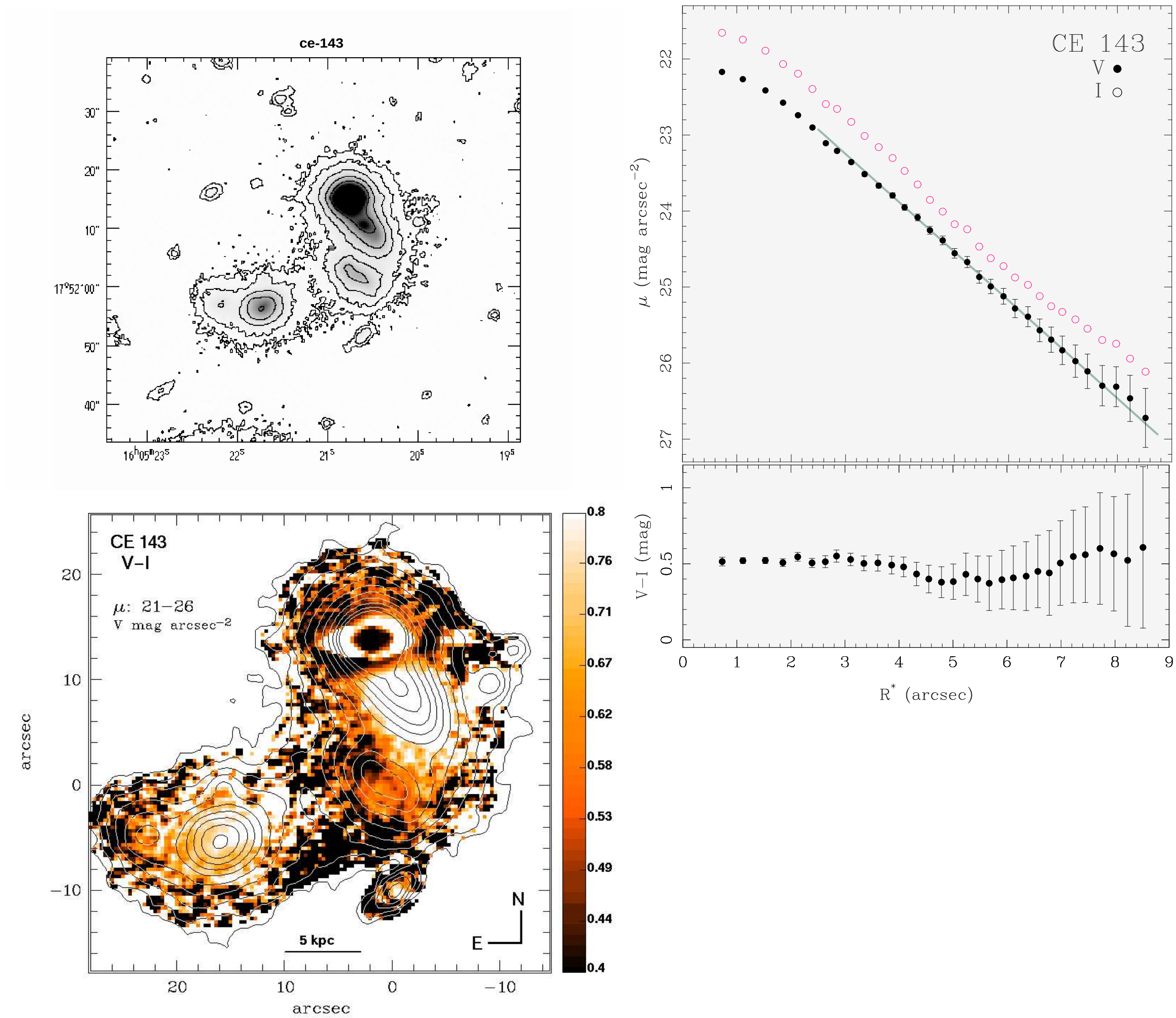

Fig. 9. Same as Figure 5 for ce-143. Due to strong overlapping with close by objects, a 2-D model was fitted and subtracted from the original images in order to be able to disentangle the light of the H I-rich dwarf. Large uncertainties are expected in the SBP for $\mu_V > 25$ mag arcsec^{-2}.

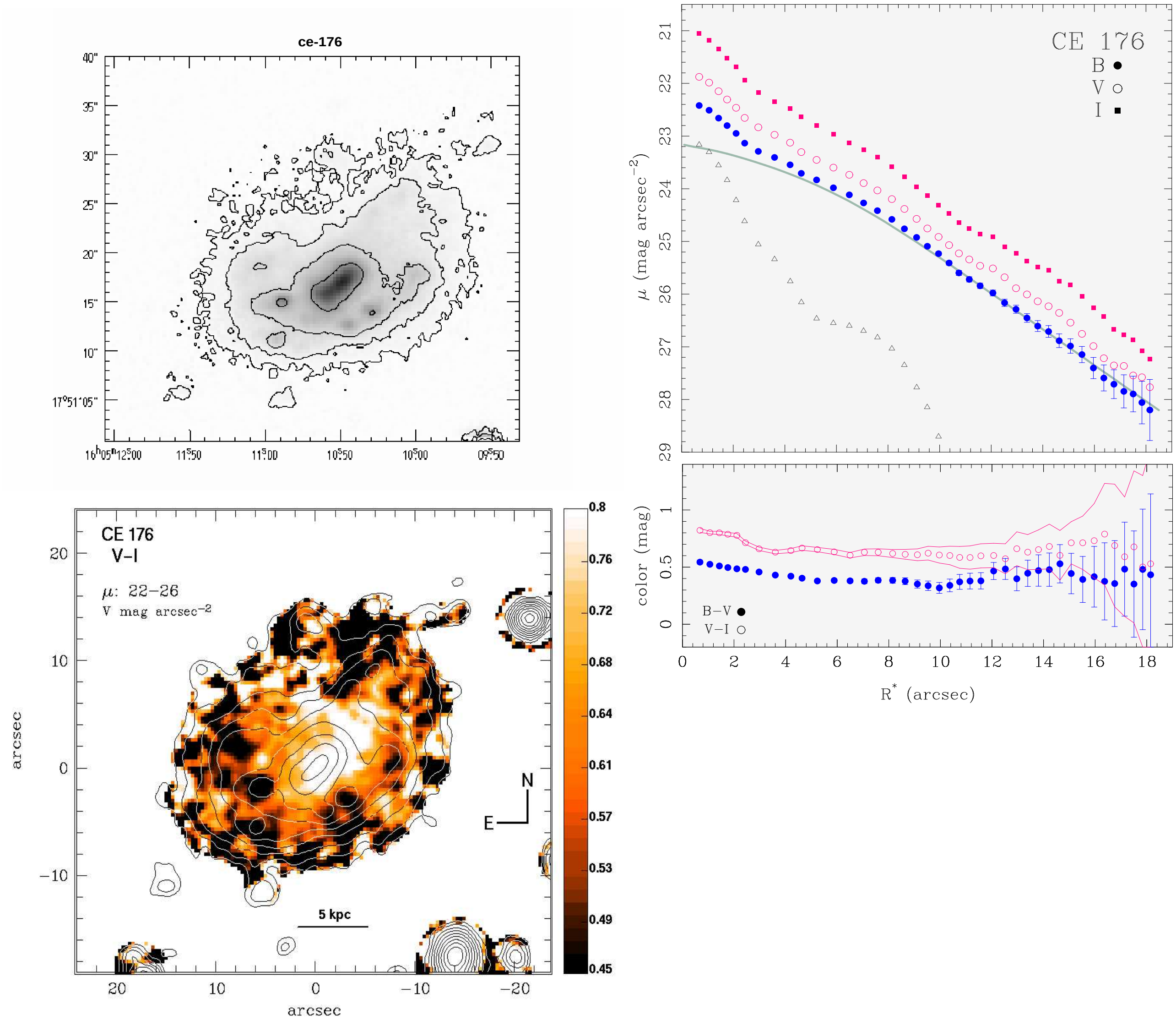

Fig. 10. Same as Figure 5 for ce-176

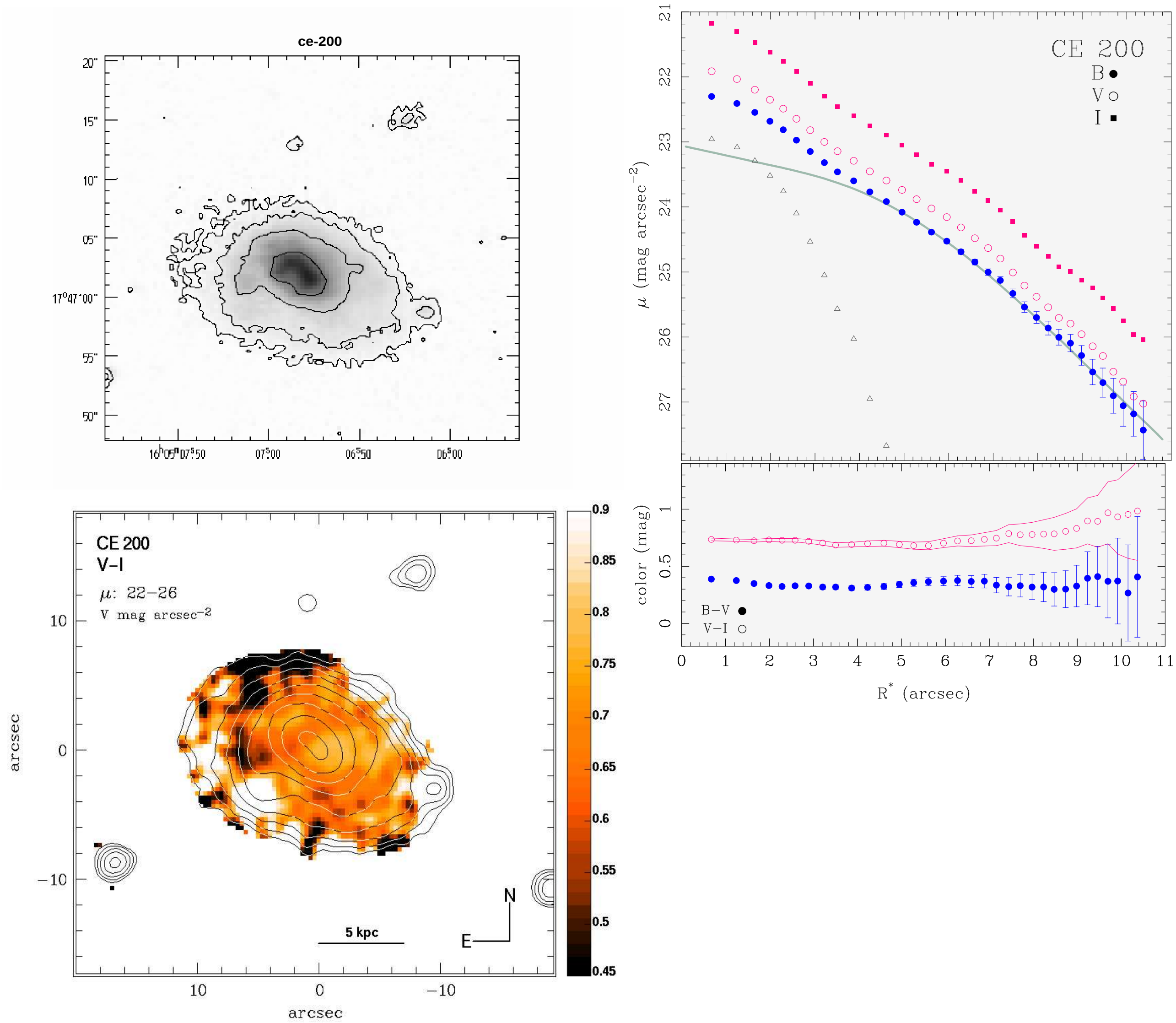

Fig. 11. Same as Figure 5 for ce-200

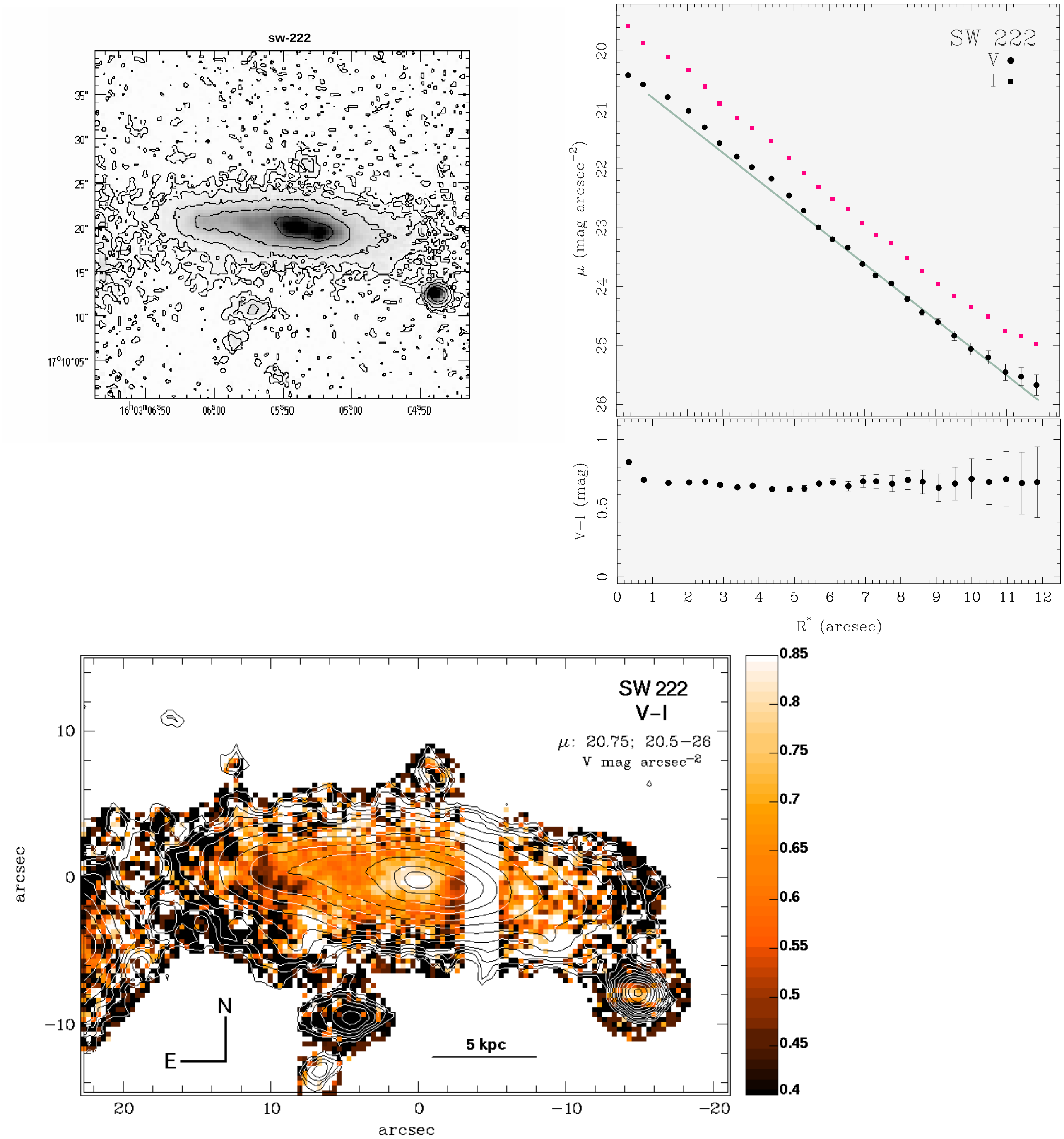

Fig. 12. Same as Figure 5 for sw-222

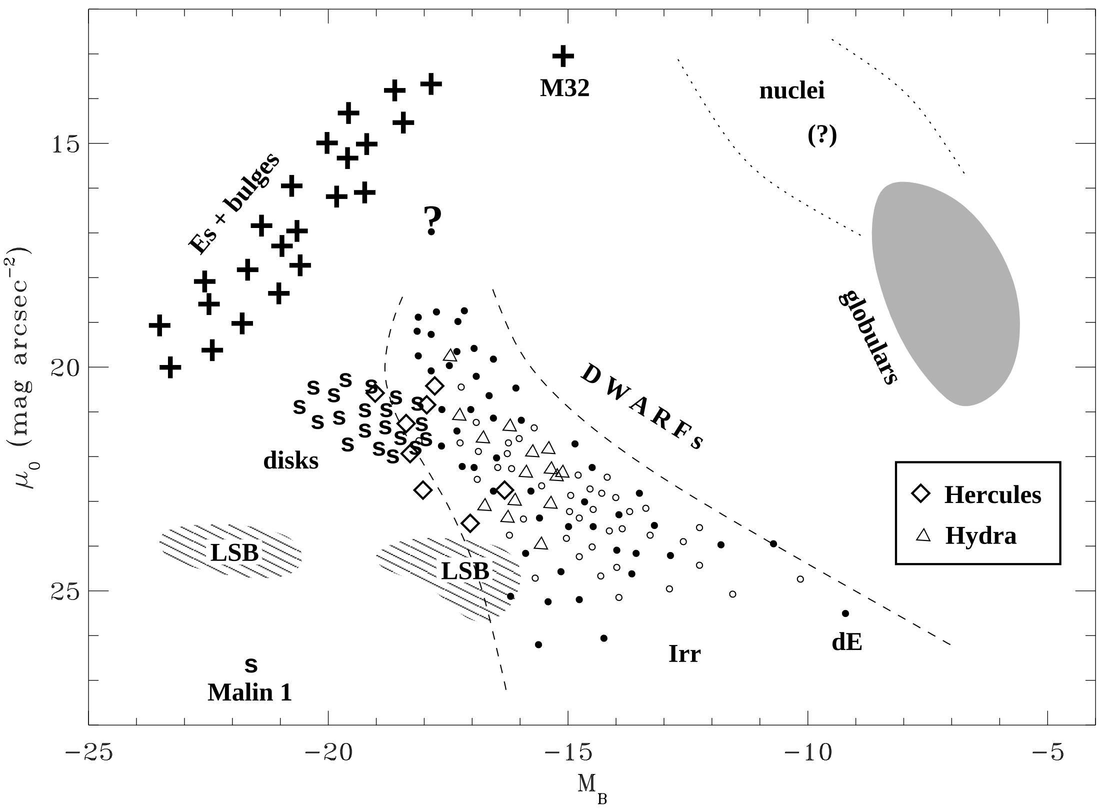

Fig. 13. Comparison of the absolute blue magnitude and the blue central surface brightness of different types of galaxies and stellar subsystems, see text for details. To the original version of Binggeli (1994) the loci of the LSB galaxies from van der Hulst (1998) have been added, as well as the boundary boxes for our sample of Hercules cluster galaxies with optical CCD surface photometry (solid lines) and the Hydra cluster dwarfs (dashed lines).

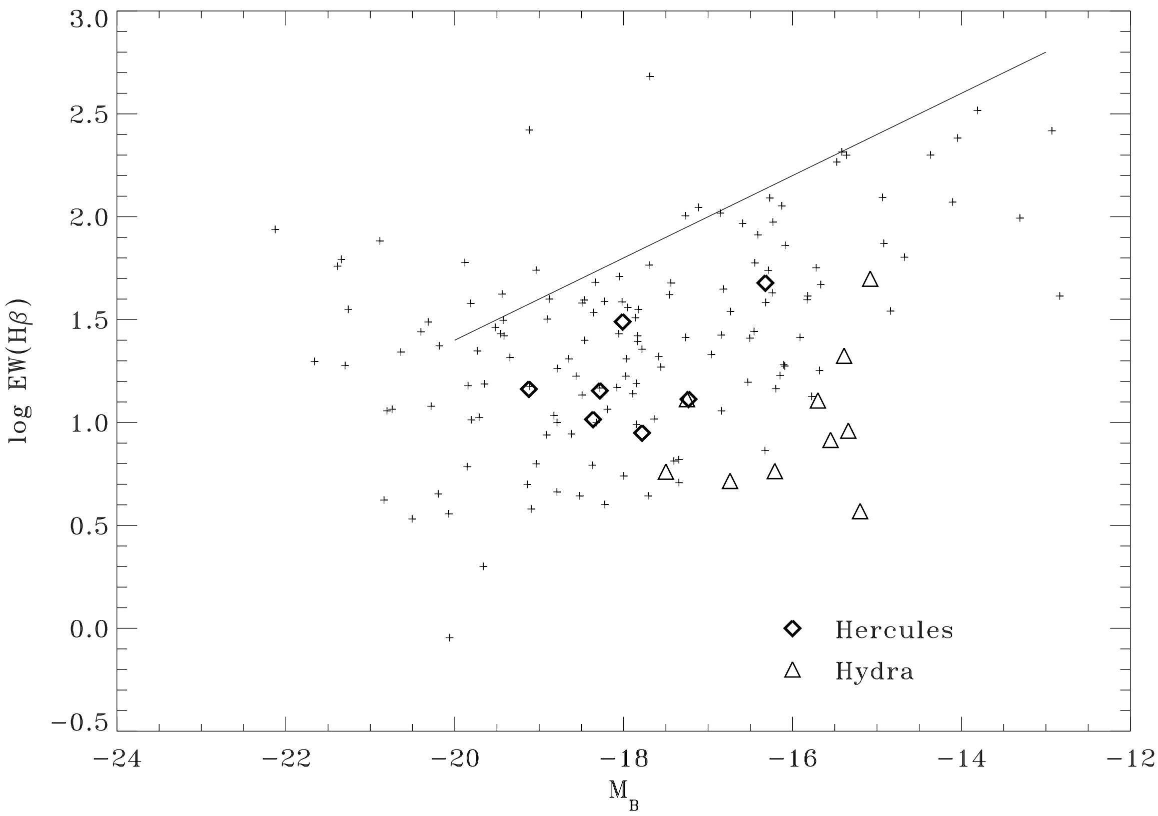

Fig. 14. M_B magnitude vs. Hβ equivalent width for the Hercules and Hydra cluster dwarfs. Open diamonds and open triangles represent the Hercules and Hydra galaxies respectively. For comparison we have also added the emission line galaxies from Salzer et al. (1989), represented by small crosses. The straight line corresponds to the eyeball upper envelope given by Vílchez (1995).

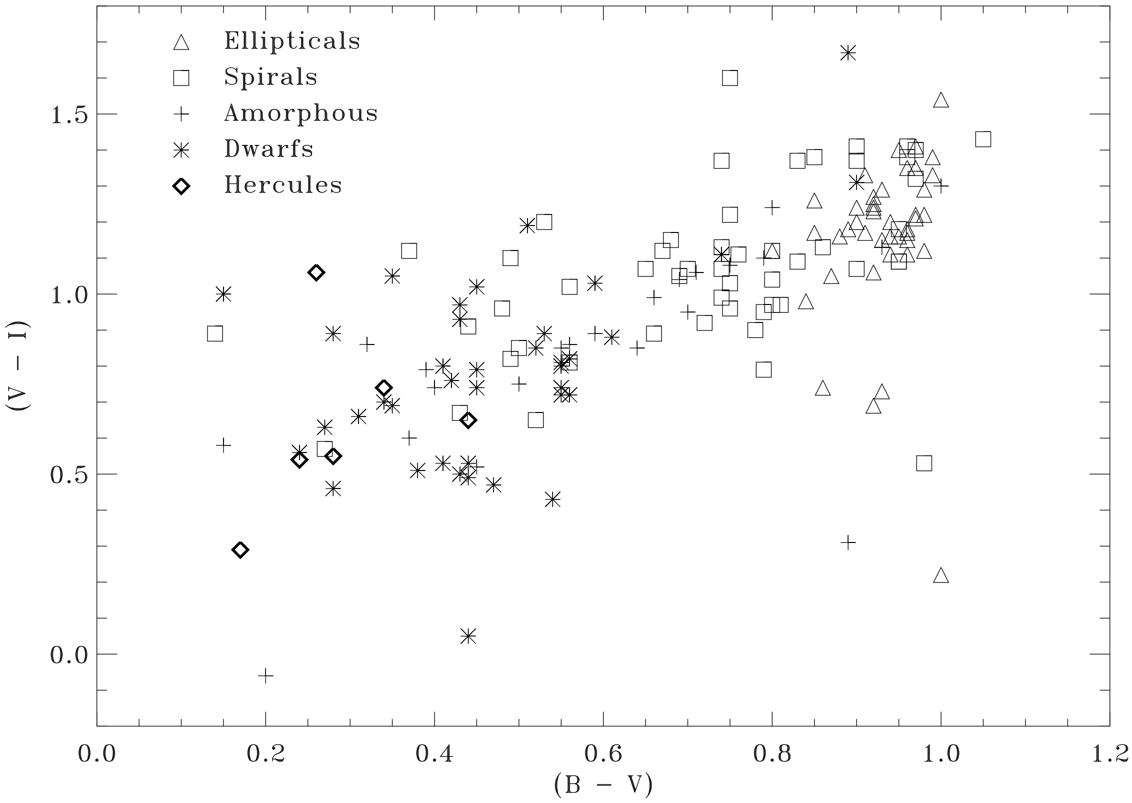

Fig. 15. $(B-V)$ *vs.* $(V-I)$ diagram for the Hercules cluster galaxies (open diamonds). Also ellipticals from Goudfrooij et al. (1994), spirals from Heraudeau & Simien (1996), amorphous galaxies from Gallagher & Hunter (1987) and nearby dwarfs from Makarova (1999) have been represented, with triangles, squares, crosses and asterisks, respectively.

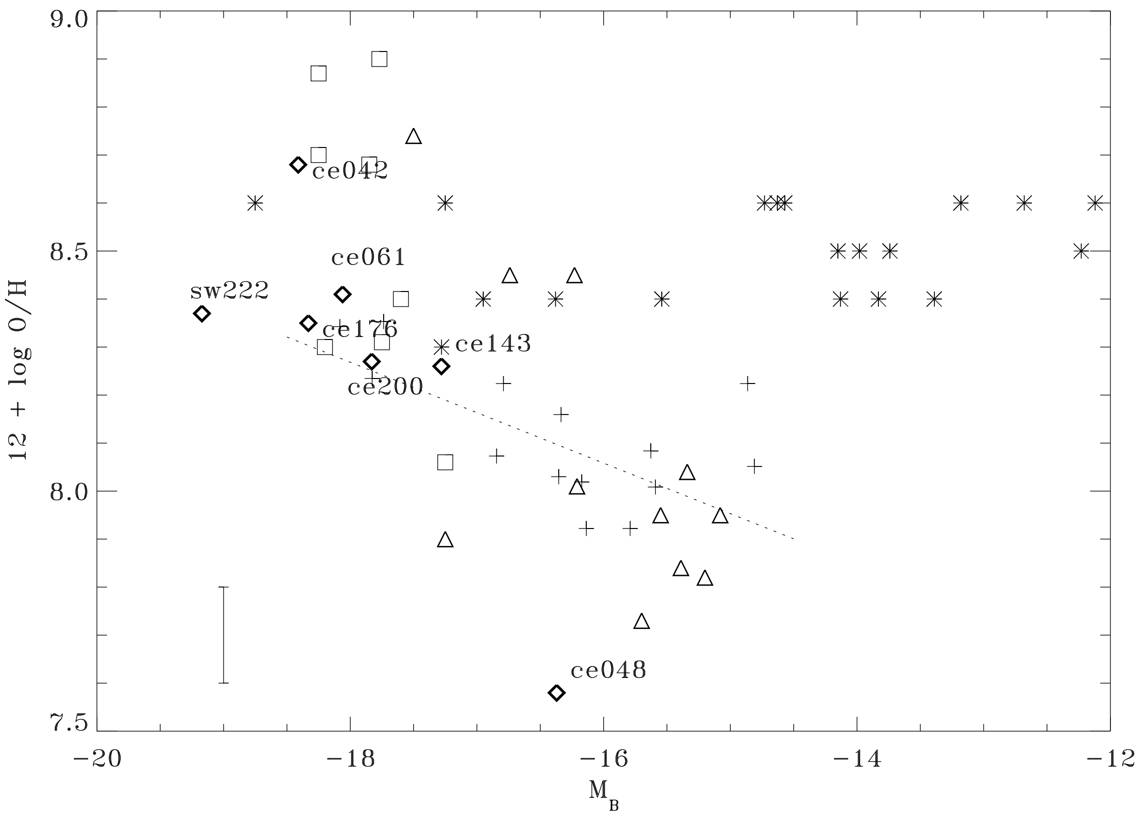

Fig. 16. Metallicity vs. luminosity relationship for the Hercules and Hydra cluster galaxies, represented by open diamonds and open triangles respectively. The typical uncertainty in the metallicity determinations is represented by the error bar at the bottom left. We have also added the sample of dwarfs from Richer & McCall (1995), the LSBs from van der Hulst et al. (1998) and the tidal dwarfs from Duc et al. (2000), represented respectively by crosses, squares and asterisks.

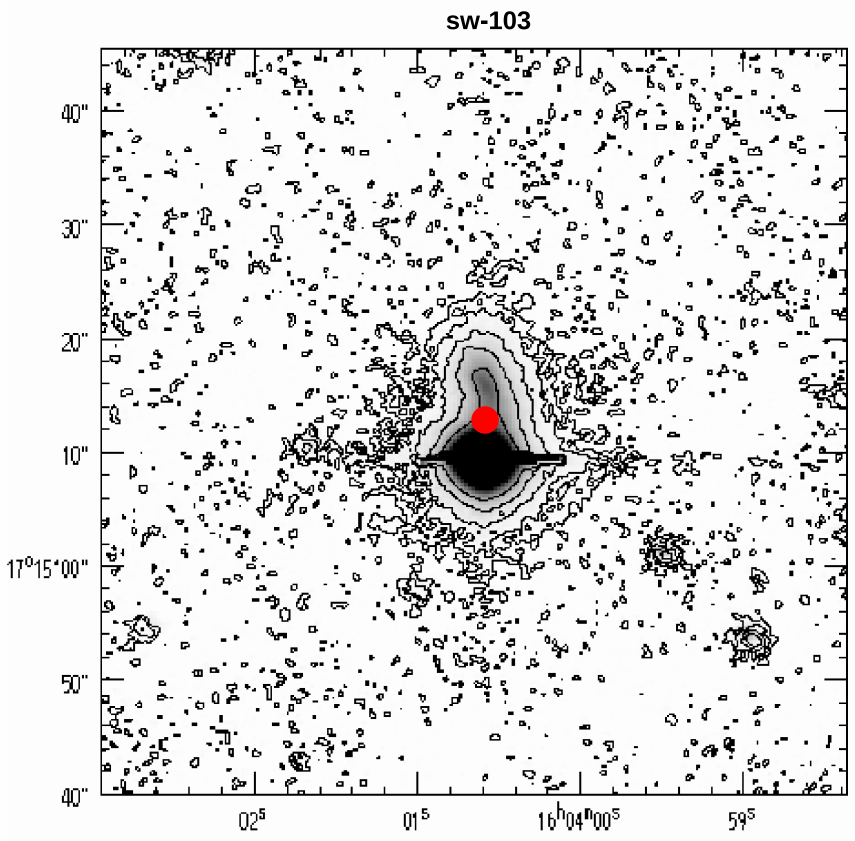

Fig. 17. (a) V-band image of the tentative detection corresponding to sw-103. Contour levels are 25.5, 24.5, 23.5, 22.5 and 21.5 mag arcsecs^{-2}. The filled circle shows the position of the HI detection.

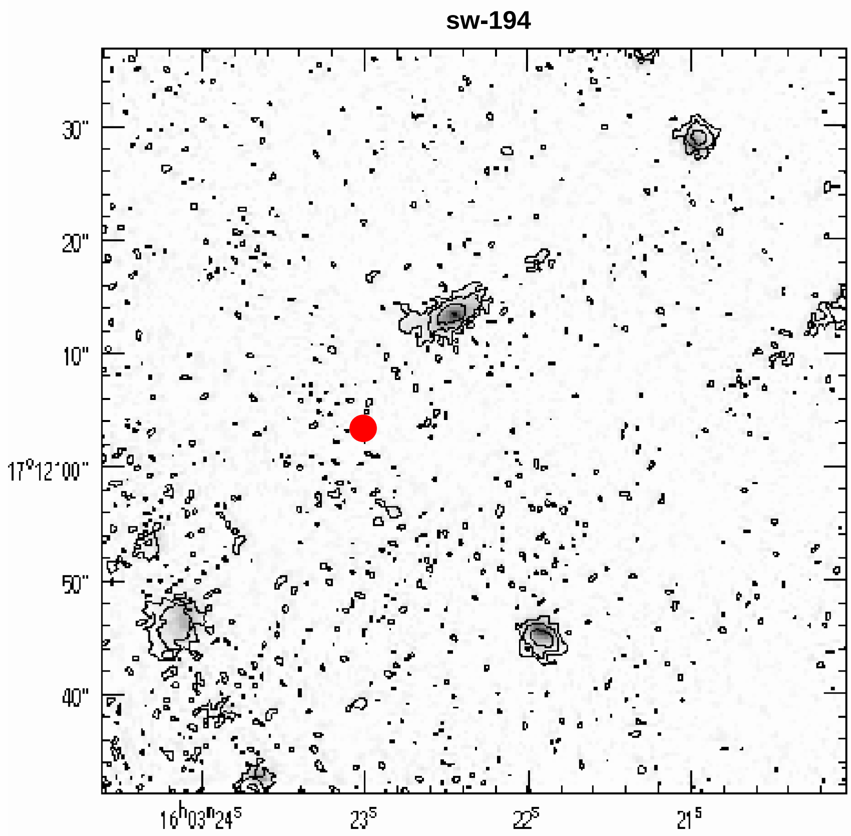

Fig. 17. (b) V-band image of the tentative detection corresponding to sw-194. Contour levels are 25.5, 24.5, 23.5, 22.5 and 21.5 mag arcsecs^{-2}. The filled circle shows the position of the HI detection.